



## Multistage-aging process effect on formation of GP zones and mechanical properties in Al–Zn–Mg–Cu alloy

Rong-xian YANG<sup>1,2</sup>, Zhi-yi LIU<sup>1,2</sup>, Pu-you YING<sup>1,2</sup>, Jun-lin LI<sup>1,2</sup>, Liang-hua LIN<sup>1,2</sup>, Su-min ZENG<sup>1,2</sup>

1. Key Laboratory of Nonferrous Metal Materials Science and Engineering, Ministry of Education, Central South University, Changsha 410083, China;
2. School of Materials Science and Engineering, Central South University, Changsha 410083, China

Received 6 March 2015; accepted 28 September 2015

**Abstract:** The tensile properties and fatigue behavior of an Al–Zn–Mg–Cu alloy were investigated by performing tensile tests and fatigue crack propagation (FCP) tests. The tensile results show that lower aging temperature modified retrogression and re-aging (RRA) process enhances the elongation, but reduces the strength of the alloy, as compared to conventional RRA process which employs peak aging temperature. Both ductility and strength, however, are increased by employing a natural aging prior to re-aging based on the former modified RRA process. Fatigue test results show that both routes reduce FCP rate. Especially, the lower re-aging temperature modified RRA process obtains the lowest FCP rate. Natural aging treatment could enhance the nucleation rate of GP zones. A large amount of GP zones could be cut by dislocations, which is responsible for the highest tensile strength and elongation, as well as lower FCP rate.

**Key words:** Al–Zn–Mg–Cu alloy; multistage-aging process; tensile properties; fatigue property; GP zone

### 1 Introduction

Al–Zn–Mg–Cu alloys had been widely used in the transport, commercial airliners, and military cargo for structural components due to their high specific strength and high fatigue crack propagation (FCP) resistance in the appropriate aged condition [1]. The precipitation sequence of Al–Zn–Mg–Cu alloys was normally understood to be: supersaturated solid solution (SSS) → coherent GP zones →  $\eta'$  phase (semi-coherent precipitates) → stable precipitates [2]. The excellent mechanical properties depended on the fine precipitates and their precursors [3]. The hardenable aluminum alloys provided high tensile strength under T6 treatment but prone to stress corrosion cracking (SCC). Then, the over-aging heat treatment T7X had been invented to improve SCC resistance because the microstructure was the stable precipitates ( $\text{MgZn}_2$ ) segregated at grain boundaries. But the tensile strength of the alloy in T7X treatment decreased obviously in comparison with that in T6 treatment because of the coarser precipitates and

wider precipitates-free zones (PFZs) [4].

In order to substantially increase the SCC resistance of Al–Zn–Mg–Cu alloys without sacrificing its maximum strength, a new heat treatment called retrogression and re-aging (RRA) was invented by Cina in 1970s. RRA treatment consisted of three steps [5,6]: First of all, pre-aged at low temperature after solution treatment (T6); secondly, retrogressed at high temperature for a short time; finally, re-aged at low temperature (T6). After the samples were aged with RRA treatment, the microstructure of Al–Zn–Mg–Cu alloy consisted of GP zones and fine  $\eta'$  phase within grain interiors similar to T6 treatment and  $\eta$  phase at grain boundaries similar to T7X treatment [4,7,8]. Later, much attention had been paid to the effect of RRA treatment on fatigue behavior. CHEN et al [7] investigated the influence of precipitates on the FCP rate of AA7055 alloy under different aging treatments. The results showed that T77-tempered sample possessed the best FCP resistance due to the shearable particles in the matrix. Furthermore, CHEN et al [3] pointed out that a narrow PFZ was beneficial to the FCP resistance. WANG

**Foundation item:** Project (51171209) supported by the National Natural Science Foundation of China; Project (2012CB619506) supported by the National Basic Research Program of China; Project supported by the 2011 Program of Nonferrous Metals and Materials, China

**Corresponding author:** Zhi-yi LIU; Tel: +86-731-88836011; E-mail: [liuzhiyi@csu.edu.cn](mailto:liuzhiyi@csu.edu.cn)  
DOI: 10.1016/S1003-6326(16)64221-8

et al [8] compared the fatigue crack growth behaviors between RRA-tempered sample and T7451-treated sample. The results indicated that dislocations cut the small coherent particles to localize slip into a single-planar variant and glided more or less reversibly during cyclic loading. This planar-reversible slip was reported to promote fatigue crack growth resistance by favoring crack deflection, crack tip closure and reducing damage accumulation [8].

More recently, multistage-aging treatments had been applied to Al–Cu–Mg–Ag and Al–Zn–Mg–Cu alloys [9–11]. LUMLEY et al [10] claimed that T6i6 condition enhanced the fraction of dispersive small size precipitates in aluminum alloys, resulting in better mechanical properties. BUHA et al [9] revealed that T6i4 treatment could simultaneously improve the tensile strength, ductility and fracture toughness. But T6i4/T6i6 treatment costs too much time at lower temperatures. And it was not fit for all aluminum alloys because of the difference in the physical properties of precipitates formed during interruption [12].

Positron annihilation lifetime spectroscopy (PALS) experiment had been utilized in Al–Zn- and Al–Zn–Mg-based alloys to study the precipitation kinetics [13–16]. FERRAGUT et al [14] combined positron annihilation spectroscopy (PALS) with Vickers microhardness to investigate the decomposition process of Al–Zn–Mg alloys. It could be concluded that the vacancies with Mg atoms were stable, and Mg-vacancies were the structural components of GP zones in the samples which were treated with natural aging after solution treatment. LIAO et al [17] demonstrated that Cu addition promoted the precipitation of Mg and Zn and increased the amount of precipitates. FERRAGUT et al [13,15] also proposed that Mg-vacancies which evolved to GP zones were dominant diffusing species under natural aging temper after solution treatment of Al–Zn–Mg–Cu alloys. This study was not only restricted to Al–Zn–Mg-based alloys, but also in other systems such as Al–Cu–Mg alloys. According to coincidence Doppler broadening (CDB) results in Ref. [18], the vacancy was prone to combine with Al atom after quenching, but the Al-vacancy fraction would decrease, both Mg-vacancy and Cu-vacancy fractions would increase instead after 150 °C, 60 s aging treatment. Then, in the subsequent condition (aging at room temperature for 48 h), the vacancies were likely to combine with Mg and Al atoms, rather than Cu atoms, and the increase in the positron lifetime with Mg alloying indicated that more Mg atoms could form vacancy complexes.

As generally known, a combination of ultrahigh strength with high ductility in aluminum alloys is contradictory. In order to improve the ductility of the ultrahigh strength aluminum alloy, purification method to

decrease the impurity content of Fe and Si is widely used. However, this method will increase the manufacturing cost. So, a new process method should be invented to improve the ductility and FCP resistance without reducing the strength of the ultrahigh strength aluminum alloys, in spite of high content of Fe and Si impurities. In Al–Zn–Mg–Cu alloy, GP zones are not only strengthening particles, but also can be sheared by moving dislocations. A shearable GP zone could be cut by dislocations [8], so it does not reduce the free-slipping distance of dislocations, leading to an increased plastic ductility. Concurrently, GP zones can give a significant strengthening effect due to boundary strengthening effect, order strengthening effect. Also, the shearable GP zones never obstruct the reversible dislocation slipping in the plastic deformation zone at fatigue crack tip, leading to high FCP resistance [7]. This suggested that GP zones are able to concurrently enhance the plastic elongation and strength, as well as FCP resistance in aluminum alloys.

Consequently, in order to improve the ductility and FCP resistance without reducing the tensile strength of an Al–Zn–Mg–Cu alloy with relatively high content of Fe and Si, the present work designs a new multistage-aging method to raise GP zone nucleation rate by employing the vacancy migration effect, and to narrow PFZs by shortening retrogression time.

## 2 Experimental

The material used in this study was Al–Zn–Mg–Cu alloy with relatively high contents of Fe and Si, and Cr-dispersoid strengthening. Its chemical composition was listed in Table 1. The materials were received as a  $d50$  mm extruded rods, and then cut them into 2 mm plates. The samples were treated at 470 °C for 1 h, then water quenched. After that, these samples were treated by three different approaches. And the detailed processes were shown in Table 2.

**Table 1** Chemical composition of investigated alloys (mass fraction, %)

Zn	Mg	Cu	Cr	Fe	Si	Al
6.28	2.19	1.6	0.15	0.4–0.6	0.4–0.6	Bal.

**Table 2** Experimental procedures of three RRA treatments

Condition	Experimental process
RRA1	470 °C, 1 h + Water quenching + 120 °C, 24 h + 200 °C, 6 min + Water quenching + 120 °C, 24 h
RRA2	470 °C, 1 h + Water quenching + 100 °C, 24 h + 200 °C, 6 min + Water quenching + 80 °C, 34 h
RRA3	470 °C, 1 h + Water quenching + 100 °C, 24 h + 200 °C, 6 min + Water quenching + natural aging (25 °C) for 10 h + 80 °C, 34 h

The tensile tests of the samples were performed on CSS 44100 universal testing machine at room temperature with 2 mm/min loading speed in long transverse (LT) direction. FCP test was carried out on compact tension (CT) specimens taken from the extruded rods in the LT orientation with the size of 45.6 mm × 38 mm × 2.5 mm ( $L \times W \times B$ ) to obtain the FCP rates. All FCP tests were conducted at a stress ratio ( $R$ ) of 0.1 with a sine-wave loading frequency of 10 Hz on an MTS machine at room temperature in laboratory air environment. Three samples were used per condition for tensile and FCP rate tests. The tensile fracture surfaces of the specimens were analyzed by a FEI Quanta 200 scanning electron microscope (SEM) with the operating voltage of 15 kV. A Tecnai G<sup>2</sup>20 transmission electron microscope (TEM) with voltage of 200 kV, along with selected area electron diffraction (SAED) was utilized to characterize the microstructure of the specimens. The samples for TEM test were prepared by mechanically grinding each side to 100 μm and punched into 3 mm discs and electro-polished by using twin-jet equipment in a mixture of 70% methanol and 30% nitric acid at -25 °C. The differential scanning calorimetry (DSC) tests were carried out on NETZSCH STA 499C with high purity aluminum as reference, the size of samples was  $d5$  mm × 0.5 mm. The heating rate in the test was 20 °C/min. Two samples were used per condition for DSC tests. The protective gas is Ar.

### 3 Results

#### 3.1 Mechanical properties

Table 3 illustrates the tensile properties of the samples in three different RRA treatments (RRA1, RRA2 and RRA3). Comparison of the tensile properties in Table 3 reveals that the RRA1-treated sample possesses the lowest elongation (11.1%) and intermediate tensile strength (674 MPa), the RRA2-treated sample shows an intermediate elongation (12.5%), but the lowest tensile strength (662 MPa), and the RRA3-treated sample possesses both the highest elongation (13.2%) and the highest tensile strength (680 MPa). According to Table 2, the RRA1-treated sample was subjected to 120 °C, 24 h peak pre-aging and 120 °C, 24 h peak re-aging. In this tempered condition, the sample generally shows the lowest elongation. The RRA2-treated sample was processed at a lower pre-aging temperature (100 °C) and re-aging temperature (80 °C), in comparison with the RRA1-treated sample. Evidently, the lower aging temperature gave rise to the increased elongation (12.5%) and degradation of tensile strength (662 MPa). The RRA3-treated sample employed an additional natural aging (25 °C, 10 h) prior to re-aging

treatment on the ground of RRA2 process. This suggests that the additional natural aging process is responsible for the concurrent increase of the elongation (13.2%) and the tensile strength (680 MPa), in comparison with RRA2-treated sample, as shown in Table 3.

**Table 3** Mechanical properties in different RRA conditions (The deviations of ultimate strength and yield strength are ±8 MPa, the deviation of elongation is ±0.4%)

Temper	Ultimate strength/MPa	Yield strength/MPa	Elongation/%
RRA1	674	649	11.1
RRA2	662	610	12.5
RRA3	680	621	13.2

The variation of FCP rates ( $da/dN$ ) with the stress intensity factor range ( $\Delta K$ ) of three RRA-treated samples is given in Fig. 1. At low  $\Delta K$  (12 MPa·m<sup>1/2</sup>), the FCP rates of all three RRA-treated samples vary in the same range. However, the three RRA-treated samples show distinctly different FCP behavior, as  $\Delta K$  increases. Especially at high  $\Delta K$  ( $\geq 20$  MPa·m<sup>1/2</sup>), RRA1-treated sample shows the highest FCP rate, RRA2-treated sample shows the lowest one, and RRA3-treated sample corresponds to the intermediate one. Additionally, the  $\Delta K$  value of RRA1-treated sample, corresponding to stable fatigue crack propagation region (Paris regime), is the smallest among all three RRA-treated samples. In contrast, that of RRA2-treated sample is the greatest, while the intermediate corresponds to RRA3-treated sample. Combination of the FCP behavior shown in Fig. 1 with RRA process parameters listed in Table 2 suggests that lower pre-aging and re-aging temperatures are beneficial to the FCP resistance, and natural aging prior to re-aging slightly decreases the FCP resistance.

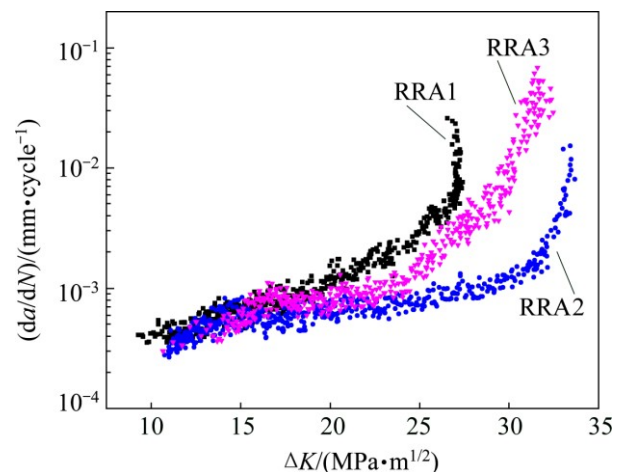


**Fig. 1** Fatigue crack propagation rates  $da/dN$  as function of stress intensity factor range  $\Delta K$  in various aging conditions

### 3.2 Microstructural characterization and DSC result

Representative fracture surfaces in different treatments are present in Fig. 2. It shows that numerous large shear zones and a small quantity of shallow dimples exist in Fig. 2(a). It is apparent that the amount of dimples increases and the size of the shear zones reduces in Fig. 2(b). This indicates that decreasing the aging temperature is beneficial to the ductility. In Fig. 2(c), the number of dimples is the largest, and the size of shear zones is the smallest. This implies that combination of lower aging temperature with natural

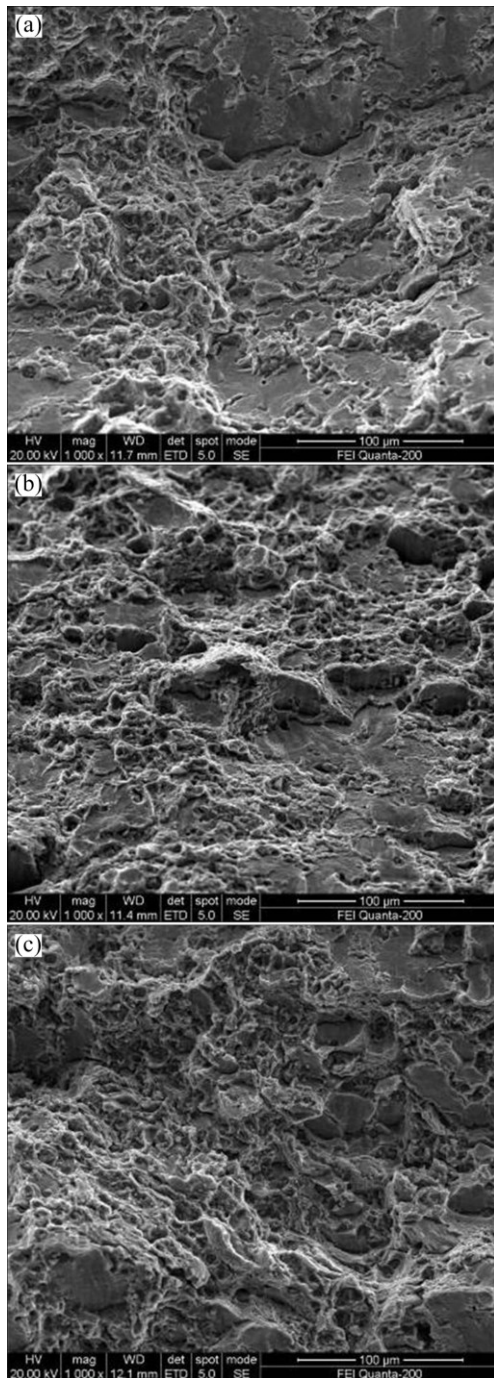


**Fig. 2** Fracture surface analysis in various conditions: (a) RRA1; (b) RRA2; (c) RRA3

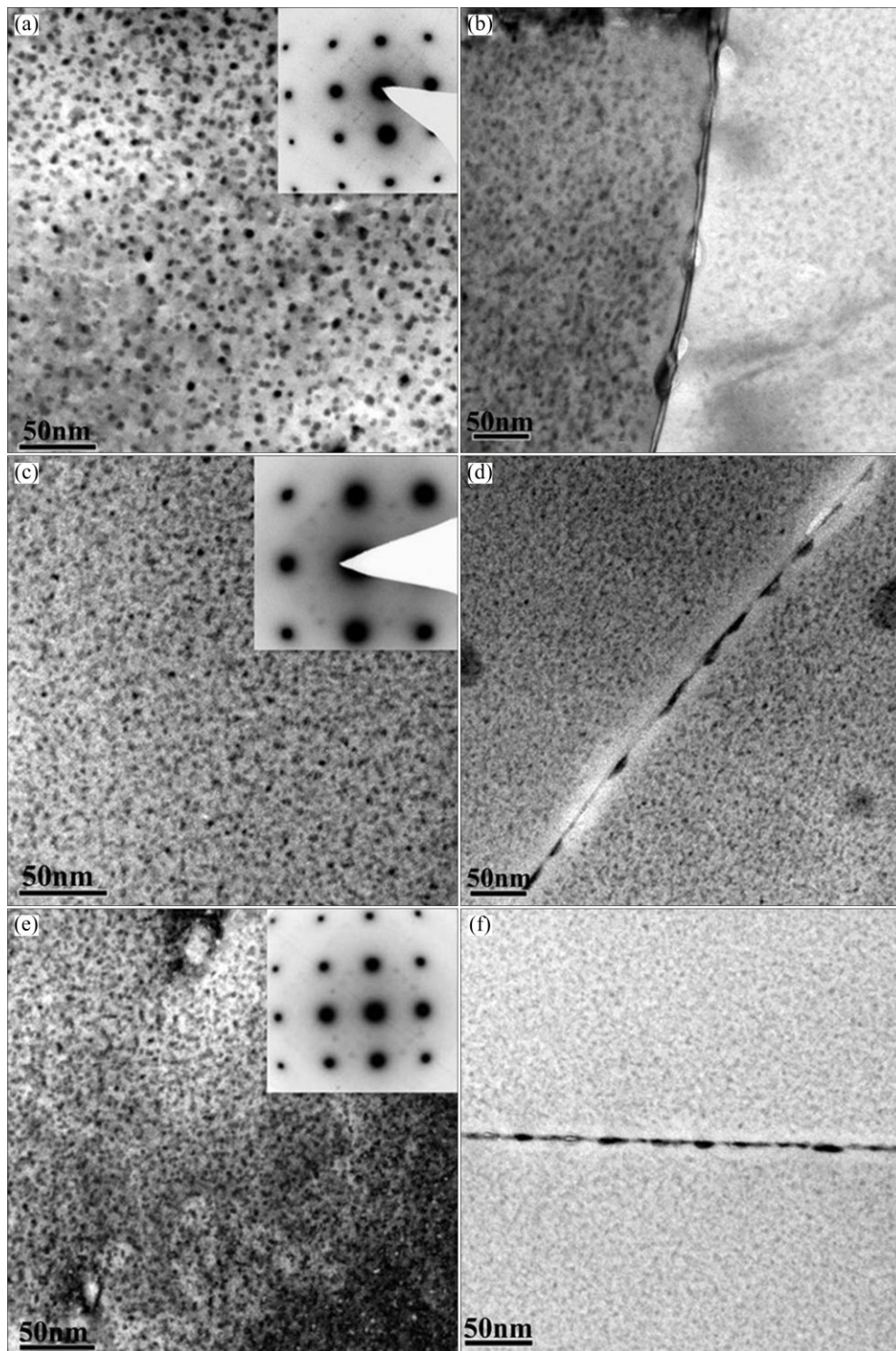
aging prior to re-aging, has advantages in improving the ductility. Comprehensive analysis of Fig. 2 reveals that the best ductility can be obtained with RRA3 treatment.

Figure 3 shows the TEM microstructures and corresponding SAED patterns in three different RRA conditions. Figure 3(a) shows that larger  $\eta'$  phase distributes uniformly within grain interiors and the spots of  $\eta'$  phase and GP zones are observed clearly. The GP zones are formed on  $\{100\}$ -planes. However,  $\eta'$  phases are formed on  $\{111\}$ -planes and the spots are brighter than those of GP zones. This indicates that  $\eta'$  phase and GP zones simultaneously exist in the RRA1-treated specimen, but the dominant second-phase particle is  $\eta'$  phase. In contrast, the spots of GP zones and  $\eta'$  phase are weak in Fig. 3(c). This is because the size of second-phase particles decreases in the RRA2-treated specimens. The microstructure in Fig. 3(e) shows that more GP zones distribute uniformly within grain interiors, and the corresponding SAED patterns show the weakest spots of  $\eta'$  phase, indicating that the  $\eta'$  phase is less and smaller. The morphologies of grain boundaries in various conditions are shown in Figs. 3(b), (d) and (f). The width of PFZs in different conditions is narrow and nearly the same due to the uniform process of retrogression.

DSC scan is utilized in conjunction with TEM observation to investigate the precipitation and dissolution processes during multistage aging treatments. Figure 4 shows a series of DSC scans of the specimens in different conditions. The first endothermic peak corresponds to the dissolution of clusters and GP zones [9,19–21], which is referred to as peak 1. The second endothermic peak corresponds to the dissolution of  $\eta'$  phase [9,21], which is referred to as peak 2. The size of peak 1 in RRA1 is the smallest, which means that the amount of GP zones in RRA1-treated sample is less than that in other samples. By comparing the size of peak 1 in RRA2 and RRA3 conditions, it shows that peak 1 in the curve of RRA3 treatment is larger than that of RRA2 treatment, indicating that more clusters and GP zones dissolve into the matrix in the RRA3-treated sample. It suggests that the largest amount of GP zone is formed during RRA3 process, as compared to RRA1 and RRA2 treatments. As to peak 2, it indicates that the  $\eta'$  phase dissolves at about 200 °C. So when the samples retrogress at 200 °C, the GP zones and  $\eta'$  phase will dissolve into the matrix. And this is the reason for choosing 200 °C as the retrogression temperature.

## 4 Discussion

Generally, two strengthening mechanisms of secondary particles have been investigated: Orowan by-passing mechanism and dislocation shearing mechanism [22,23]. The decomposition of supersaturated



**Fig. 3** TEM microstructures and corresponding SAED patterns taken in  $\langle 001 \rangle$  zone axis under different treatments: (a, b) RRA1; (c, d) RRA2; (e, f) RRA3

solid solution of an Al-3.2%Zn-2.2%Mg alloy has been investigated in Ref. [24]. UNGÁR et al [24] found that between 20 and 70 °C, the precipitation process of Al-Zn-Mg alloy was the nucleation and growth of GP zones. And between 100 and 160 °C, the precipitation process of the alloy was the formation of  $\eta'$  phase. This indicates that GP zones are the dominant precipitates

with the re-aging temperature of 80 °C and  $\eta'$  phase is the dominant precipitate with the re-aging temperature of 120 °C. After the shearable particles (GP zones and finer  $\eta'$  phase [25,26]) being cut by the dislocations, the resistance of precipitates to the mobile dislocations is decreased, and the free-slipping distance of dislocations increases. As a result, the ductility will improve

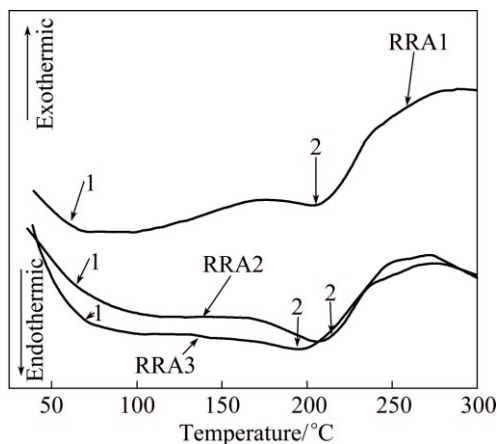


Fig. 4 DSC scans carried out on Al-Zn-Mg-Cu alloy in various treatments

obviously. On the contrary, the dislocation has to bypass the large  $\eta'$  phase. With the increase of dislocation loops, the interparticle distance will be reduced and the mobile dislocations bow-out between the particles will be harder. In the RRA2-treated sample, the precipitates are GP zones and fine  $\eta'$  phase, and the amount of GP zones is larger than that of RRA1-treated sample. On this account, RRA2-treated sample exhibits lower strength and higher ductility. Then from Figs. 3 and 4, a fact has been revealed that numerous GP zones are served as the main strengthening phase in RRA3-treated sample. And the effect of natural aging after solution treatment has been investigated by PALS in Al-Zn-Mg-based alloys [13–15]. During natural aging process, spherical particles corresponding to solute clusters or GP zones with the sizes smaller than 2 nm are formed, and no  $\eta'$  phase appears [13]. In this study, the precipitates formed during pre-aging process dissolve into the matrix in the retrogression process. Supersaturated vacancies are prone to combine with Mg atoms instead of Cu atoms during natural aging process [14]. This will accelerate the diffusion of Mg atom, and increase the nucleation rate of GP zones because Mg-vacancy is the structural component of GP zones. As a result, the total quantities of particles in RRA3-treated sample are the largest of all samples, as shown in Fig. 4. So, the tensile strength of RRA3-treated sample is higher than that of other two RRA-treated samples. In addition, the GP zones and shearable small size  $\eta'$  phase can be cut by moving dislocations, resulting in the increase of free-slipping distance of dislocations, and finally the enhancing of the ductility.

Then, as to the FCP resistance, the RRA1-treated sample possesses the highest FCP rates due to the un-shearable particles within grain interiors. And the

RRA2-treated sample possesses the lowest FCP rates at high  $\Delta K$  ( $\geq 20 \text{ MPa}\cdot\text{m}^{1/2}$ ). This is because GP zones and shearable  $\eta'$  phase exist within grain interiors. SRIVATSAN [27] explained that the shearable particles would be cut by the dislocation into a smaller size and gradually decomposed in Al-Zn-Mg-Cu alloy. Progressive decomposition of the shearable precipitates resulted from the to-and-fro motion of the moving dislocations cause the weakened plane to continue to slip and the deformation to become localized [27]. Because the GP zones dissolution is easier than shearable  $\eta'$  phase by repeated cutting of moving dislocations, the FCP rate of RRA3-treated sample is higher than that of RRA2-treated sample. This is consistent with the explanation of cyclic softening in Al-Cu-Mg alloys, which ascribes the cyclic softening to the small Cu-Mg co-clusters becoming unstable during the repeated cutting by moving dislocations and beginning to dissolve as the cyclic loading continued [28]. And numerous studies have been carried out in 2000 and 7000 series aluminum alloys, in order to investigate the influence of microstructures on the FCP rate [29–32]. Our previous study, which will be published elsewhere, investigated the FCP resistance of the Al-Cu-Mg alloy in different conditions. The results show that the FCP resistance of 170 °C, 8 h tempered sample is higher than that of T351 and 170 °C, 0.5 h tempered samples. This indicates that larger co-cluster and semi-coherent  $S'$  phase within grain interiors can decrease the FCP rates as compared to small size co-clusters.

## 5 Conclusions

1) Among all the multistage-aging processed samples, the RRA2-treated sample exhibits the highest FCP resistance, intermediate elongation and the lowest tensile strength, due to the GP zones and shearable  $\eta'$  phase formed in low temperature pre-aging and re-aging conditions.

2) The RRA3-processed sample possesses both the highest elongation and tensile strength, as well as intermediate FCP resistance. It is because natural aging prior to re-aging treatment promotes the formation of clusters and GP zones, leading to the largest amount of precipitates, and the dominant GP zones present in RRA3-treated samples.

## References

- [1] STARKE E A Jr, STALEY J T. Application of aluminum alloys to aircraft [J]. Prog Aerospace Sci, 1996, 32(2): 131–172.

- [2] WANG Tao, YIN Zhi-min, SHEN Kai, LI Jie, HUANG Ji-wu. Single-aging characteristics of 7055 aluminum alloy [J]. Transactions Nonferrous Metals Society of China, 2007, 17(3): 548–552.
- [3] CHEN Xu, LIU Zhi-yi, LIN Mao, NING Ai-lin, ZENG Su-min. Enhanced fatigue crack propagation resistance in an Al–Zn–Mg–Cu alloy by retrogression and re-aging treatment [J]. J Mater Eng Perform, 2012, 21(11): 2345–2353.
- [4] SHE Huan, CHU Da, WANG Jun, SUN Bao-de. Effects of silicon content on microstructure and stress corrosion cracking resistance of 7050 aluminum alloy [J]. Transactions Nonferrous Metals Society of China, 2014, 24(7): 2307–2313.
- [5] NING Ai-lin, LIU Zhi-yi, PENG Bei-shan, ZENG Su-min. Redistribution and re-precipitation of solute atom during retrogression and reaging of Al–Zn–Mg–Cu alloys [J]. Transactions Nonferrous Metals Society of China, 2007, 17(5): 1005–1011.
- [6] FENG Chun, LIU Zhi-yi, NING Ai-lin, LIU Yan-bin, ZENG Su-min. Retrogression and re-aging treatment of Al–9.99%Zn–1.72%Cu–2.5%Mg–0.13%Zr aluminum alloy [J]. Transactions Nonferrous Metals Society of China, 2006, 16(5): 1163–1170.
- [7] CHEN Jun-zhou, ZHEN Liang, YANG Shou-jie, DAI Sheng-long. Effects of precipitates on fatigue crack growth rate of AA 7055 aluminum alloy [J]. Transactions Nonferrous Metals Society of China, 2010, 20(12): 2209–2214.
- [8] WANG Yi-lin, PAN Qing-lin, WEI Li-li, LI Bo, WANG Ying. Effect of retrogression and reaging treatment on the microstructure and fatigue crack growth behavior of 7050 aluminum alloy thick plate [J]. Mater Des, 2014, 55(4): 857–863.
- [9] BUHA J, LUMLEY R N, CROSKY A G. Secondary ageing in an aluminum alloy 7050 [J]. Mater Sci Eng A, 2008, 492(1): 1–10.
- [10] LUMLEY R N, POLMEAR I J, MORTON A J. Interrupted aging and secondary precipitation in aluminum alloys [J]. Mater Sci Technol, 2003, 19(11): 1483–1490.
- [11] FERRAGUT R, DUPASQUIER A, MACCHI C E, SOMAZA A, LUMLEY R N, POLMEAR I J. Vacancy–solute interactions during multiple-step ageing of an Al–Cu–Mg–Ag alloy [J]. Scripta Mater, 2009, 60(3): 137–140.
- [12] RISANTI D D, YINM CASTILLA DEL P D, ZWAAG DER S V. A systematic study of the effect of interrupted ageing conditions on the strength and toughness development of AA6061 [J]. Mater Sci Eng A, 2009, 523(1–2): 99–111.
- [13] FERRAGUT R, SOMOZA A, TOLLEY A. Microstructural evolution of 7012 alloy during the early stages of artificial aging [J]. Acta Mater, 1999, 47(17): 4355–4364.
- [14] FERRAGUT R, SOMOZA A, DUPASQUIER A. On the two-step ageing of a commercial Al–Zn–Mg alloy—A study by positron lifetime spectroscopy [J]. J Phys: Condens Matter, 1996, 8(45): 8945–8952.
- [15] FERRAGUT R, SOMOZA A, DUPASQUIER A. Positron lifetime spectroscopy and decomposition processes in commercial Al–Zn–Mg-based alloys [J]. J Phys: Condens Matter, 1998, 10(17): 3903–3918.
- [16] ABIS S, BIASINI M, DUPASQUIER A, SFERLAZZO P, SOMOZA A. Positron annihilation study of  $\eta'$  precipitation kinetics in an aluminum alloy [J]. J Phys: Condens Matter, 1989, 1(23): 3679–3686.
- [17] LIAO Yu-guo, HAN Xiao-qi, ZENG Miao-xia, JIN Man. Influence of Cu on microstructure and tensile properties of 7XXX series aluminum alloy [J]. Mater Des, 2015, 66(2): 581–586.
- [18] MARCEAU R K W, SHA G, FERRAGUT R, DUPASQUIER A, RINGER S P. Solute clustering in Al–Cu–Mg alloys during the early stages of elevated temperature ageing [J]. Acta Mater, 2010, 58(15): 4923–4939.
- [19] SALAMCI E. Calorimetric and transmission electron microscopy studies of spray deposited Al–Zn–Mg–Cu alloys [J]. Mater Sci Technol, 2004, 20(7): 859–863.
- [20] PINK E, WEBERNIG W M. Guinier-Preston zones and the onset strain of serrated flow [J]. Mater Sci Eng, 1987, 93: L1–L4.
- [21] LOFFLER H, KOVACS I, LENDVAI J. Review decomposition processes in Al–Zn–Mg alloys [J]. J Mater Sci, 1983, 18(8): 2215–2240.
- [22] DORIN T, GEUSER DE F, LEFEBVRE W, SIGLI C, DESCHAMS A. Strengthening mechanisms of  $T_1$  precipitates and their influence on the plasticity of an Al–Cu–Li alloy [J]. Mater Sci Eng A, 2014, 605: 119–126.
- [23] QUEYREAU S, MONNET G, DEVINCRE B. Orowan strengthening and forest hardening superposition examined by dislocation dynamics simulations [J]. Acta Mater, 2010, 58(17): 5586–5595.
- [24] UNGAR T, LENDVAI J, KOVACS I, GROMA G, KOVACS-CSETENYI E. The decomposition of the solid solution state in the temperature range 20 to 200 °C in an Al–Zn–Mg alloy [J]. J Mater Sci, 1979, 14(3): 671–679.
- [25] CHEN Jun-zhou, ZHEN Liang, YANG Shou-jie, SHAO Wen-zhu, DAI Sheng-long. Investigation of precipitation behavior and related hardening in AA 7055 aluminum alloy [J]. Mater Sci Eng A, 2009, 500(1–2): 34–42.
- [26] LIU Yan, JIANG Da-ming, LI Bing-qing, YANG Wen-shu, HU Jie. Effect of cooling aging on microstructure and mechanical properties of an Al–Zn–Mg–Cu alloy [J]. Mater Des, 2014, 57: 79–86.
- [27] SRIVATSAN T S. Mechanisms governing cyclic deformation and failure during elevated temperature fatigue of aluminum alloy 7055 [J]. Int J Fatigue, 1999, 21(6): 557–569.
- [28] BAI Song, LIU Zhi-yi, ZHOU Xuan-wei, GU Yan-xia, YU Di-er. Strain-induced dissolution of Cu–Mg co-clusters and dynamic recrystallization near a fatigue crack tip of an underaged Al–Cu–Mg alloy during cyclic loading at ambient temperature [J]. Scripta Mater, 2011, 64(12): 1133–1136.
- [29] LIU Zhi-yi, LI Fu-dong, XIA Peng, BAI Song. Mechanisms for Goss-grains induced crack deflection and enhanced fatigue crack propagation resistance in fatigue stage II of an AA2524 alloy [J]. Mater Sci Eng A, 2015, 625: 271–277.
- [30] BAI Song, LIU Zhi-yi, GU Yang-xia. Microstructures and fatigue fracture behavior of an Al–Cu–Mg–Ag alloy with a low Cu/Mg ratio [J]. Mater Sci Eng A, 2011, 530: 473–480.
- [31] BAI Song, LIU Zhi-yi, LI Yun-tao. Microstructures and fatigue fracture behavior of an Al–Cu–Mg–Ag alloy with addition of rare earth Er [J]. Mater Sci Eng A, 2010, 527(7–8): 1806–1814.
- [32] LIU Yan-bin, LIU Zhi-yi, LI Yun-tao, XIA Qin-kun, ZHOU Jie. Enhanced fatigue crack propagation resistance of an Al–Cu–Mg alloy by artificial aging [J]. Mater Sci Eng A, 2008, 492(1–2): 333–336.

## 多级时效处理对 Al-Zn-Mg-Cu 合金 GP 区形成及力学性能的影响

杨荣先<sup>1,2</sup>, 刘志义<sup>1,2</sup>, 应普友<sup>1,2</sup>, 李俊霖<sup>1,2</sup>, 林亮华<sup>1,2</sup>, 曾苏氏<sup>1,2</sup>

1. 中南大学 有色金属材料科学与工程教育部重点实验室, 长沙 410083;

2. 中南大学 材料科学与工程学院, 长沙 410083

**摘要:** 通过拉伸性能和疲劳裂纹扩展试验研究 Al-Zn-Mg-Cu 合金的拉伸性能和疲劳性能。拉伸试验结果显示, 与利用峰时效温度的传统回归再时效(RRA)相比, 较低时效温度的 RRA 处理能够提高合金的伸长率, 但是降低了合金的强度。但是, 在前面改良的 RRA 处理基础上, 在再时效之前增加自然时效, 可以同时提高合金的强度和塑性。疲劳测试结果显示, 两条改良的工艺路线都可以降低疲劳裂纹扩展速率。尤其是采用较低再时效温度改良的 RRA 工艺获得最低的疲劳扩展速率。自然时效处理提高了 GP 区的形核速率。大量的 GP 区都能够被位错切割。因此该状态合金拥有最高的强度和伸长率, 以及较低的疲劳裂纹扩展速率。

**关键词:** Al-Zn-Mg-Cu 合金; 多级时效工艺; 拉伸性能; 疲劳性能; GP 区

(Edited by Yun-bin HE)